

# RSC Advances



This is an *Accepted Manuscript*, which has been through the Royal Society of Chemistry peer review process and has been accepted for publication.

*Accepted Manuscripts* are published online shortly after acceptance, before technical editing, formatting and proof reading. Using this free service, authors can make their results available to the community, in citable form, before we publish the edited article. This *Accepted Manuscript* will be replaced by the edited, formatted and paginated article as soon as this is available.

You can find more information about *Accepted Manuscripts* in the [Information for Authors](#).

Please note that technical editing may introduce minor changes to the text and/or graphics, which may alter content. The journal's standard [Terms & Conditions](#) and the [Ethical guidelines](#) still apply. In no event shall the Royal Society of Chemistry be held responsible for any errors or omissions in this *Accepted Manuscript* or any consequences arising from the use of any information it contains.

## Reaching beyond HIV/HCV: Nelfinavir as a potential starting point for broad-spectrum protease inhibitors against dengue and chikungunya virus

Soumendranath Bhakat<sup>a\*</sup>, Leen Delang<sup>b</sup>, Suzanne Kaptein<sup>b</sup>, Johan Neyts<sup>b\*</sup>, Pieter Leyssen<sup>b</sup>, Venkatesan Jayaprakash<sup>c\*</sup>

<sup>a</sup> Division of Biophysical Chemistry, Lund University, P.O. Box 124, SE-22100 Lund, Sweden

<sup>b</sup> KU Leuven – University of Leuven, Department of Microbiology and Immunology, Rega Institute for Medical Research, Laboratory of Virology and Chemotherapy, B-3000 Leuven, Belgium

<sup>c</sup> Department of Pharmaceutical Sciences and Technology, Birla Institute of Technology, Mesra-835215, India

\*Corresponding authors

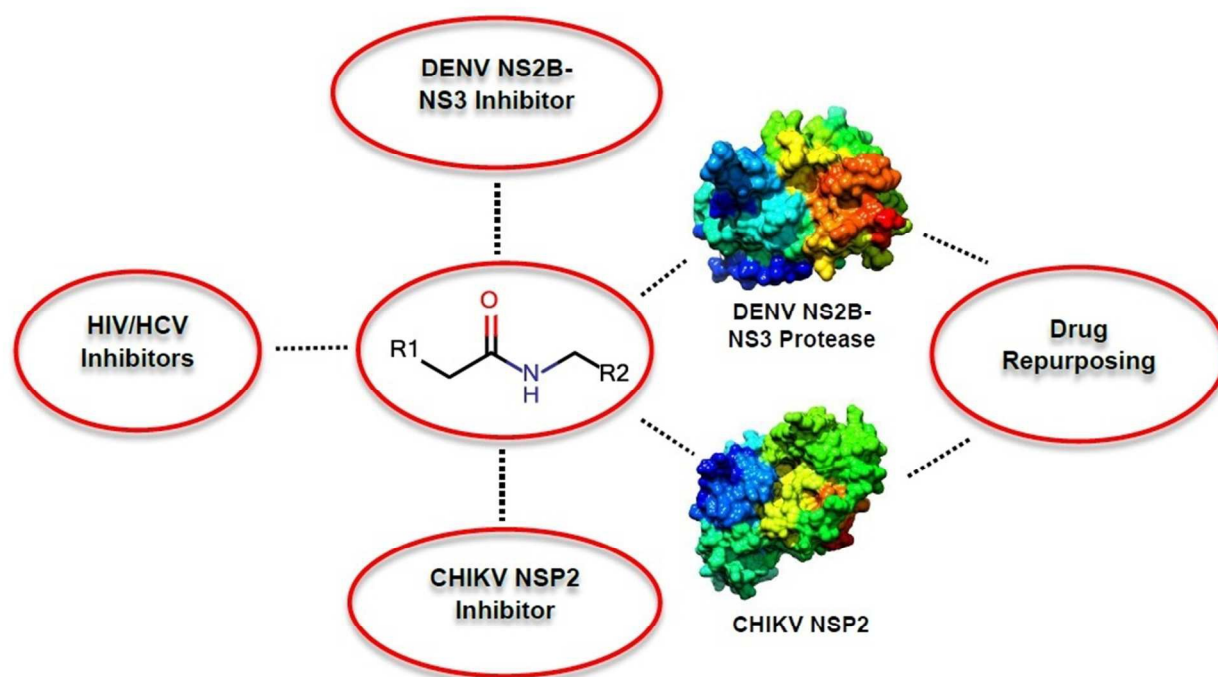
Soumendranath Bhakat; email: [soumendranath.bhakat@bpc.lu.se](mailto:soumendranath.bhakat@bpc.lu.se)

Johan Neyts; email: [johan.neyts@rega.kuleuven.be](mailto:johan.neyts@rega.kuleuven.be)

Venkatesan Jayaprakash; email: [venkatesanj@bitmesra.ac.in](mailto:venkatesanj@bitmesra.ac.in)

**Running title:** Repositioning of HIV/HCV Inhibitors

## Graphical Abstract



## Abstract

Drug repurposing or re-profiling has become an effective strategy to identify novel indications for already-approved drugs. In this study, peptidomimetic FDA-approved HIV/HCV inhibitors were explored for their potential to be repurposed for the inhibition of the replication of dengue (DENV) and chikungunya virus (CHIKV) by targeting the NS2B-NS3 and NSP2 protease, respectively. MM/GBSA-based binding free energy results put nelfinavir forward as potential inhibitor of both dengue and chikungunya virus, which subsequently was further explored in a virus-cell-based assay for both viruses. Nelfinavir showed modest antiviral activity against CHIKV ( $EC_{50} = 14 \pm 1 \mu\text{M}$  and a selectivity index of 1.6) and was slightly more active against DENV-2 ( $EC_{50} = 3.5 \pm 0.4 \mu\text{M}$  and a selectivity index of 4.6). Even though the antiviral potency was limited, the fact that some activity was observed in these assays made it worth to explore the potential and properties of nelfinavir as a step-stone compound: a more detailed computational analysis was performed to understand the binding mode, interaction, hydrogen bond distance, occupancy and minimum pharmacophoric features. The comprehensive data set that resulted from these analyses may prove to be useful for the development of novel DENV and CHIKV protease inhibitors.

**Keywords:** Dengue virus; chikungunya virus; protease inhibitors, drug repurposing; nelfinavir



## 1. Introduction

The discovery and development of novel chemical entities from scratch into a drug for clinical use is a time- and money-consuming effort(1-3). Therefore, there is a lot of truth in the famous quote by Nobel laureate James Black: “*The most fruitful basis of the discovery of a new drug is to start with an old drug*”(1). Taking these words to heart, there is still a lot of potential in the many compounds that are currently on the market and for which it is still unknown how they exactly elicit their beneficial effect. Furthermore, also for drugs with a known mechanism, it still makes sense to explore their versatility. Antiviral drug development for neglected tropical diseases is considered to be challenging because of their low market value, in spite the increasing need (4-6). Drug repositioning or re-profiling(7-10) may be an attractive and effective process to unlock the clinical potential of established molecules for the treatment of neglected tropical diseases such as dengue (DENV) and chikungunya virus (CHIKV)(11-14).

Dengue and chikungunya virus are the two most prevalent tropical mosquito-borne diseases that affect humans (15, 16). Cases have even been reported on the concurrent transmission of both viruses amongst travelers(15). DENV (genus *Flavivirus*, family *Flaviviridae*) is endemic in more than 100 countries with an average annual global incidence of 390 million cases, of which around 96 million develop dengue disease (*Bhatt et al.*, 2013(17)). In general, DENV infection follows a subclinical course that is characterized by non-specific symptoms. However, a second infection with any of the other four DENV serotypes is strongly correlated with the clinically more severe dengue hemorrhagic fever (DHF) and dengue shock syndrome (DSS)(18, 19). Various vaccine development programs are already ongoing for several years(20, 21), but this proves to be quite challenging due to the link between secondary infection and the underlying mechanism of DHF/DSS, i.e. antibody-dependent enhancement of infection. Patients those who

suffer from DENV disease can only be offered symptomatic treatment and intensive care(18). CHIKV belongs to the *Alphavirus* genus of the *Togaviridae* family(22, 23). This viral infection is mostly characterized by acute and chronic articular manifestations. Although CHIKV infection is rarely fatal, the disease evolves into a chronic stage in ~50% of the infected patients and is characterized by persistent disabling polyarthrititis that can severely incapacitate the patient for weeks up to several years beyond the acute stage(24). Despite its wide spread and high morbidity, at the moment, there is no approved vaccine or antiviral treatment available(22). The administration of analgesics, antipyretics, and anti-inflammatory agents is the only way to increase the comfort of the patient.

For viruses, the non-structural (NS) viral proteins are attractive targets for the design of drug-like molecules(15). A lot of information, like the crystal structure, is available for proteases, which, for other viruses, has already proven to facilitate the development of peptidomimetic inhibitors. The hydrophobic NS2B part is essential for the activation of the DENV NS3, which contains the catalytic triad His51, Asp75 and Ser135 within its N-terminal region (**Figure 1**). For CHIKV, NSP2 (**Figure 2**), which carries three catalytic cysteine residues (Cys1233, Cys1274 and Cys1290) in its C-terminal region as well as four histidine residues (His1222, His1228, His1229 and His136), is also a potential target for the development of peptidomimetic inhibitors(15, 22).

### **Figure 1**

### **Figure 2**

The HIV/HCV protease inhibitors (25-27) (**Figure 3**), benchmark examples of peptidomimetic inhibitors, target the enzymatic activity of the respective viral proteases. Building on this knowledge, extensive studies have been performed to develop peptidomimetic inhibitors that

target the DENV NS2B-NS3 (**Figure 5**) or CHIKV NSP2 protease (**Figure 4**). Because all these inhibitors share common structural features (**Figure 6**), it prompted us to explore whether HIV/HCV protease inhibitors could possibly be re-purposed for the inhibition of the replication of DENV and CHIKV.

**Figure 3**

**Figure 4**

**Figure 5**

**Figure 6**

In this report, computer-aided drug design (CADD) and enhanced molecular modeling techniques were used to investigate whether HIV/HCV protease inhibitors that are already on the market could have the potential to inhibit the replication of DENV and CHIKV by exploration of their capacity to bind to the viral NS2B-NS3 or NSP2 protease, respectively. In parallel, their biological potency was evaluated in virus-cell-based assays and was correlated with the *in silico* results.

## **2. Materials and Methods**

### **2.1. Molecular Modeling Study**

The crystal structure of the DENV NS2B-NS3 protease in its ligand bound conformation (PDB: 3U1I)(28) and the CHIKV NSP2 protease (PDB: 3TRK)(29) was obtained from the protein data bank. The closed conformation of the DENV NS2B-NS3 subunit (PDB: 3U1I)(28) was preferred over the open conformation without ligand (PDB: 2FOM)(30) as the protease is presumed to remain in a closed conformation when bound to an inhibitor. The structures of the HIV/HCV protease inhibitors that were used in this study were procured from Chemspider database(31) and

downloaded in MOL2 format. The receptor and ligands were prepared as mentioned previous by *Maharaj et al*(32). Subsequently, processed ligands were docked in the active site of the DENV NS2B-NS3 and CHIKV NSP2 protease using Autodock Vina(33). The top docked conformations were generated using ViewDock(34) plugin integrated with Chimera(35).

Molecular docking-based binding affinity calculation often leads to artifacts. Therefore, further molecular dynamics analysis was used for further refinement. Molecular dynamics-based MM/GBSA calculation (36-40) has proven to be an effective tool to re-rank protein-inhibitor binding affinity. Therefore, molecular dynamics based MM/GBSA rescoring (36, 41-43) was used to precisely rank the HIV/HCV inhibitors against both target enzymes.

All molecular dynamics simulations were performed using the GPU version of the PMEMD engine provided with Amber 14(44) as described by *Bhakat et al*(45). The H<sup>++</sup> server (<http://biophysics.cs.vt.edu/H++>) was used to assign correct protonation states in case of all the systems prior to system preparation. In brief, the ligands were parameterized using GAFF force field, whereas the protein systems were described using FF99SB force field integrated with Amber 14. The Leap module integrated with Amber 14 was used to add missing hydrogen atoms and heavy atoms as well as counter ions to neutralize the systems. All the systems were immersed in a TIP3P water box so that no atom was within 10 Å of any box edge. Long-range coulombic interactions were treated using particle mesh Ewald (PME) implemented in Amber 14. The prepared systems were then subjected to different stages e.g. minimizations, heating and equilibration before proceeding to production runs as described by *Bhakat et al*(45). Finally, a 30ns **explicit solvent** molecular dynamics simulation was performed for all the systems using an NPT ensemble with a target pressure set at 1 bar and constant pressure coupling of 2 ps.

The molecular dynamics trajectories were analyzed using PTRAJ and CPPTRAJ modules(46) integrated with Amber 14. Visualization was carried out using VMD(47) and Chimera(35).

MM/GBSA-based binding energy was calculated using a singular trajectory approach taking in account 1.000 frames with a regular interval of 30 ps(45). The following set of equations describes the calculation of binding free energy.

$$\Delta G_{\text{bind}} = G_{\text{complex}} - G_{\text{receptor}} - G_{\text{ligand}} \quad (1)$$

$$\Delta G_{\text{bind}} = E_{\text{gas}} + G_{\text{sol}} - T\Delta S \quad (2)$$

$$E_{\text{gas}} = E_{\text{int}} + E_{\text{vdw}} + E_{\text{ele}} \quad (3)$$

$$G_{\text{sol}} = G_{\text{GB}} + G_{\text{SA}} \quad (4)$$

$$G_{\text{SA}} = \gamma \text{SASA} \quad (5)$$

The notations of these parameters were described in detail by *Bhakat et al*(45).

## 2.2. DENV and CHIKV cell-based assay

### 2.2.1. Cells and virus strains

CHIKV Indian Ocean strain 899 (Genbank FJ959103.1) was generously provided by Prof. S. Günther (Bernhard Nocht Institute for Tropical Medicine, Hamburg, Germany). CHIKV was propagated in African green monkey kidney cells [Vero cells (ATCC CCL-81)]. Vero-B cells were maintained in cell growth medium composed of minimum essential medium (MEM Rega-3, Gibco, Belgium) supplemented with 10% Fetal Bovine Serum (FBS, Integro, The Netherlands), 1% L-glutamine (Gibco), and 1% sodium bicarbonate (Gibco). The antiviral assays were performed in assay medium, which is the respective cell growth medium supplemented with 2% FBS (instead of 10%). All cell cultures were maintained at 37°C in an atmosphere of 5% CO<sub>2</sub> and 95-99% humidity.

DENV serotype 2 strain New Guinea C (DENV-2 NGC) was kindly provided by Dr. V. Deubel (formerly at Institute Pasteur, Lyon, France). DENV was propagated in C6/36 mosquito cells (from *Aedes albopictus*; ATCC CCL-1660) at 28 °C in Leibovitz's L-15 medium (Life Technologies, Cat N°11415049) supplemented with 10% FBS, 1% non-essential amino acids (Life Technologies, Cat N°11140035), 1% HEPES buffer (Life Technologies, Cat N°15630056) and 1% penicillin (100 U/ml)/streptomycin (100 µg/ml) solution. Antiviral assays using DENV were performed on Vero-B cells (obtained from the European Collection of Cell Cultures) using the same assay medium as was described for CHIKV.

### 2.2.2. Chikungunya virus CPE reduction assay

CHIKV cytopathic effect (CPE) reduction assays were performed as described before (*Delang et al*, 2014(48)). In brief, Vero-B cells were seeded in 96-well tissue culture plates (Becton Dickinson, Aalst, Belgium) at a density of  $2.5 \times 10^4$  cells/well in 100 µl assay medium and were allowed to adhere overnight. Next, a compound dilution series was prepared in the medium on top of the cells after which the cultures were infected with 0.01 MOI of CHIKV 899 inoculum in 100 µl assay medium. On day 5 post-infection (p.i.), the plates were processed using the MTS/PMS method as described by the manufacturer (Promega, The Netherlands). The 50% effective concentration (EC<sub>50</sub>), which is defined as the concentration of compound that is required to inhibit viral RNA replication by 50%, was determined using logarithmic interpolation. Potential cytotoxic/cytostatic effect of the compound was quantified in uninfected cells also by means of the MTS/PMS method. The 50% cytotoxic concentration (CC<sub>50</sub>; i.e., the concentration that reduces the overall metabolic activity of the cells by 50%) was calculated using logarithmic interpolation. All assay wells were checked microscopically for minor signs of

virus-induced CPE or alterations of host cell or monolayer morphology that may have been caused by the compound.

### 2.2.3. Dengue virus yield reduction assay

Vero-B cells ( $5 \times 10^4$ ) were seeded in 96-well plates. One day later, medium was replaced by 100  $\mu$ l assay medium containing 100 CCID<sub>50</sub> (50% cell culture infectious doses) of DENV-2 and incubated for 2 hours, after which the cell monolayer was washed 3 times with assay medium to remove non-adsorbed virus. Cells were further cultivated in 200  $\mu$ l fresh assay medium containing 2-fold serial dilutions of the compounds (50 – 0.20  $\mu$ g/ml) for 4 days. Supernatant was harvested and viral RNA load was determined by real-time quantitative RT-PCR, as previously described (*Kaptein et al.*, 2010(49)). The EC<sub>50</sub> value, which is defined as the compound concentration that is required to inhibit viral RNA replication by 50%, was determined using logarithmic interpolation. Potential cytotoxic/cytostatic effects of the compounds were evaluated in uninfected cells using the MTS/PMS method similarly as was described for CHIKV.

## 3. Results and Discussions

### 3.1. Insights from MM/GBSA-based rescoring and the virus-cell-based assays

From the docking studies, it could be derived that all the selected HIV/HCV inhibitors are able to physically bind into the active site of DENV NS2B-NS3 as well as that of the CHIKV NSP2 (**Figure 7**). To validate the docking protocol, the peptide-like inhibitor complexed with DENV NS2B-NS3 protease (PDB: 3U1I(28)) was extracted in the configuration as it was bound and was re-docked into the active site of DENV serine protease (details described in Supplementary Materials). **Figure 7** highlights the binding mode of all HIV/HCV inhibitors inside the active site

of DENV NS2B-NS3 protease and CHIKV NSP2, which also highlights the preciseness of the docking protocol used in this study.

### Figure 7

Subsequently, the docked HIV/HCV protease inhibitors were subjected to molecular dynamics and post-dynamics MM/GBSA-based binding free-energy analysis to understand the binding affinity of these HIV/HCV inhibitors in the active site of the DENV NS2B-NS3 and CHIKV NSP2 protease. **Table 1** lists the MM/GBSA-based scoring profile of the respective inhibitors. The energies that were derived from different binding free-energy components such as electrostatic, van der Waals (VdW) contributions were comparatively higher in case of nelfinavir when compared to the other ligands, and this for both proteases. An interesting observation in all cases was that contributions coming from *VdW* components are significantly higher than those of electrostatic components, which signifies that *VdW* interactions are the main driving force behind the binding of HIV/HCV inhibitors into the active site of the DENV NS2B-NS3 and CHIKV NSP2 protease.

### Table 1

To explore whether the *in silico* results are predictive for antiviral activity against the respective viruses, the effect of the HIV/HCV protease inhibitors was evaluated in *in vitro* virus-cell-based assays with DENV and CHIKV. As shown in **Table 2**, most HIV/HCV protease inhibitors did not inhibit the replication of CHIKV. Only lopinavir and nelfinavir showed a modest antiviral effect (**Figure 8A**). None of the compounds fully inhibited virus-induced cytopathic effects and the antiviral activity seems to be associated with an adverse effect on the host cell (MTS

cytotoxicity assay and microscopic evaluation). Likewise, only two out of the nine HIV/HCV protease inhibitors showed some antiviral activity against DENV-2 (**Table 2**, **Figure 8B**). The antiviral activity of ritonavir is clearly associated with an adverse effect on the host cell, while the antiviral effect of nelfinavir against DENV-2 was a bit more pronounced with an  $EC_{50}$  value of  $3.5 \pm 0.4 \mu\text{M}$  and a selectivity index (SI) of 4.6 ( $SI = CC_{50}/EC_{50}$ ). In general, the antiviral effect of NFV on DENV-2 replication was better compared to few previously reported DENV inhibitors (15, 50, 51).

### Table 2

It was interesting to observe that nelfinavir, the compound which was found to be the most promising compound in the *in silico* study, also showed some antiviral activity against both viruses in cell culture, (**Table 2**). It is also necessary to mention that all HIV/HCV inhibitors displayed a better binding free energy profile in complex with DENV NS2B/NS3 protease as compared to CHIKV NSP2, which can be correlated with slightly better anti-DENV as compared to anti-CHIKV activity. A more detailed modeling analysis of nelfinavir bound in both proteases (see **section 3.2**) provided additional support that, even though the antiviral effect in cell culture was rather modest, nelfinavir showed some interesting features to further explore its properties as a step-stone towards the development of inhibitors that could inhibit both DENV and CHIKV replication.

### Figure 8

## 3.2. Molecular analysis of the nelfinavir-protease interaction

### 3.2.1. The nelfinavir/DENV NS2B-NS3 interaction

A more detailed analysis of the interaction of nelfinavir with the active site of the DENV NS2B-NS3 protease delineates a number of crucial residues involved in the interaction (**Figure 9**). The majority of the interactions are hydrophobic and polar type interactions. Also, a per-residue footprint analysis confirmed that van der Waals energy is the main driving force for binding, which is exemplified by the high VdW values in binding free-energy (**Figure 9C**). The position of three catalytic site residues e.g. His51, Asp75 and Ser135 will play a crucial role in the development of novel inhibitors using the structural features of NFV (**Figure 9B**). NFV formed two backbone hydrogen bond interactions with Met84 and one with Gly153. It also formed a *pi-pi* stacking interaction with Tyr161 and a side chain H bond interaction with Thr83 (**Figure 9A**). A molecular dynamics study highlights that Met84 and Thr83 formed a stable hydrogen bond interaction with NFV with higher % occupancy during simulation time (**Table 3**). Whereas, the % occupancy of the hydrogen bond interaction between Gly153 is lower (79.3%) as compared to the other two residues (**Table 3**). The lower % hydrogen bond occupancy in case of Gly153 can be further confirmed from the fact that the electrostatic contribution coming from Gly153 is slightly lower (~0.15 kcal/mol) when compared with Thr83. Thus, the *backbone* H-bond interaction with Met84, Gly153 and *side chain* H-bond interaction with Thr83 played a crucial role in capturing the binding orientation of NFV inside the active site of the DENV serine protease.

**Figure 9A**

**Figure 9B**

**Figure 9C**

**Table 3**

### 3.2.2. The nelfinavir/CHIKV NSP2 interaction

The binding mode of NFV with the NSP2 of CHIKV puts forward some interesting observations in terms of binding mode as well as residues that are involved. It was observed that one of the conserved cysteine residues of the catalytic triad, Cys1290, appears to be involved in the binding of NFV in the active site. In addition, NFV interacts with conserved active site residues His1222, Ser1293, Gly1176 etc. at the C-terminal domain of NSP2 (**Figure 10A**). Most importantly, the formation of a hydrogen bond between His1222 and a carbonyl moiety appears to play an important role in the stability of NFV inside the active site (**Figure 10A**). The majority of the interactions were polar and hydrophobic in nature, which correlates with the high value of *van der Waals* contributions to the total binding free-energy as well as the high contribution of *VdW* forces in the per-residue energy decomposition (**Figure 10B**). The interaction between NFV and the CHIKV NSP2 was found to be stable during the simulation time with backbone C- $\alpha$  RMSD and the potential energy of the system was found to be well converged during the period of simulation (**Figure S1**, **Figure S2**, Supplementary Materials). To understand the stability of the conserved hydrogen bond between His1222 and NFV, the H-bond distance and % occupancy between the oxygen atom of the carbonyl group and the His1222 were monitored during simulation time. From **Figure 10A**, it can be clearly stated that the hydrogen bond between these two moieties was very stable with a % occupancy of 88.2 and an average distance of 3.50 Å, which further points out the role of His1222 in the stability of NFV inside the active site (**Table 4**). The binding conformation of NFV during the simulation time in respect to conserved cysteine and histidine residues (**Figure 10C**) further gives an insight into the binding theme of NFV that

can help in understanding the development of novel CHIKV inhibitors with the NFV template as starting point.

**Figure 10A**

**Figure 10B**

**Table 4**

**Figure 10C**

### **3.3. Conclusive pharmacophore features of nelfinavir**

The pharmacophore features and hypothesis presented in **Figure 11** highlights the minimum pharmacophore requirements based on the structural template of NFV and its interaction with active site residues of DENV NS2B-NS3 and CHIKV NSP2 protease will help in the design and identification of novel protease inhibitors that target the DENV NS2B-NS3 and CHIKV NSP2. The pharmacophoric features presented in **Figure 11** can be used as a template for future pharmacophore-based drug discovery efforts and to screen large commercial databases e.g. ZINC Pharmer(52) etc. to find novel leads. Not only that: the combination of structural similarity and minimum pharmacophore features of NFV will be effective in the future to pick new inhibitors from large pools of chemical compounds to identify novel small-molecule protease inhibitors against these neglected tropical diseases.

**Figure 11**

## **4. Conclusion**

In the present study, we applied a drug re-profiling strategy to explore the antiviral effect of selected HIV/HCV inhibitors against DENV and CHIKV. The peptidomimetic scaffold of HIV/HCV inhibitors and its structural similarity with previously reported DENV NS2B-NS3 and CHIKV NSP2 protease inhibitors inspired us to re-profile HIV/HCV inhibitors against the DENV NS2B-NS3 and CHIKV NSP2 protease. MM/GBSA-based binding free energy profile analysis highlighted a better binding of nelfinavir to the DENV NS2B-NS3 and CHIKV NSP2 protease, which was further validated by a modest antiviral activity of nelfinavir on CHIKV ( $EC_{50} = 14 \pm 1 \mu\text{M}$ ) and a bit more pronounced antiviral effect on DENV-2 ( $EC_{50} = 3.5 \pm 0.4 \mu\text{M}$  and  $SI = 4.6$ ) in virus-cell-based assays. Besides nelfinavir, lopinavir displayed a modest antiviral effect against CHIKV but none of these compounds fully inhibit virus-induced cytopathic effects. Ritonavir modestly inhibited DENV-2 but its activity is clearly associated with an adverse effect on the host cells. From this study, it can be concluded that NFV has more pronounced antiviral activity against DENV-2 as compared to CHIKV. The structural and pharmacophoric features now could be used to identify novel leads from chemical databases as well as for the design of novel inhibitors that target both DENV and CHIKV. This study also gave credibility to the fact that further optimization of structural and pharmacophore features of nelfinavir may lead to development of multifunctional small-molecule inhibitor that target both the DENV NS2B-NS3 and CHIKV NSP2 protease. It is also worth to mention that previous reports highlighted anti-HCV(53) and anti-cancer properties(54) of nelfinavir. Adding to this the antiviral activity against DENV and CHIKV corroborates that nelfinavir has unique properties that endow it with activity in different systems. Thus, future efforts to understand the structural and pharmacophore features of nelfinavir that are responsible for its diverse activity will be essential to develop novel multi-functional inhibitors.

Therefore, the binding mode, interaction and pharmacophore features of nelfinavir that have been highlighted in this manuscript will not only act as a step stone to develop novel DENV and CHIKV protease inhibitors, but also may be applied to identify novel protease inhibitors that target other neglected viral diseases from large pools of small-molecule inhibitors.

## 5. Acknowledgements

SB wish to thank computational support from MSKCC cBio cluster during the academic year of 2013-15. VJ likes to acknowledge the financial and infrastructure support from Birla Institute of Technology, Mesra. We also would like to acknowledge Ruben Pholien, Annelies De Ceulaer and Caroline Collard for their excellent assistance in the generation of the antiviral data.

## 6. Conflict of Interests

Authors declare no potential academic or financial conflict of interests.

## 7. References

1. <http://www.nature.com/drugdisc/news/articles/nrd1766.html>.
2. Adams, C. P., and Brantner, V. V. (2006) Estimating the cost of new drug development: is it really 802 million dollars?, *Health Aff* 25, 420-428.
3. DiMasi, J. A., Hansen, R. W., and Grabowski, H. G. (2003) The price of innovation: new estimates of drug development costs, *J Health Econ* 22, 151-185.
4. (2008) Drug discovery for neglected diseases, *Nat Rev Drug Discov* 7, 955-955.
5. Chatelain, E., and Ioset, J.-R. (2011) Drug discovery and development for neglected diseases: the DNDi model, *Drug Design, Development and Therapy* 5, 175-181.
6. Gilbert, I. H. (2013) Drug discovery for neglected diseases: molecular target-based and phenotypic approaches, *J Med Chem* 56, 7719-7726.
7. AbdulHameed, M. D., Chaudhury, S., Singh, N., Sun, H., Wallqvist, A., and Tawa, G. J. (2012) Exploring polypharmacology using a ROCS-based target fishing approach, *J Chem Inf Model* 52, 492-505.
8. Hu, X., Compton, J. R., Abdulhameed, M. D., Marchand, C. L., Robertson, K. L., Leary, D. H., Jadhav, A., Hershfield, J. R., Wallqvist, A., Friedlander, A. M., and Legler, P. M. (2013) 3-substituted indole inhibitors against *Francisella tularensis* FabI identified by structure-based virtual screening, *J Med Chem* 56, 5275-5287.

9. Li, J., Zheng, S., Chen, B., Butte, A. J., Swamidass, S. J., and Lu, Z. (2015) A survey of current trends in computational drug repositioning, *Brief Bioinform* 31.
10. Keiser, M. J., Setola, V., Irwin, J. J., Laggner, C., Abbas, A. I., Hufeisen, S. J., Jensen, N. H., Kuijjer, M. B., Matos, R. C., Tran, T. B., Whaley, R., Glennon, R. A., Hert, J., Thomas, K. L. H., Edwards, D. D., Shoichet, B. K., and Roth, B. L. (2009) Predicting new molecular targets for known drugs, *Nature* 462, 175-181.
11. Ashburn, T. T., and Thor, K. B. (2004) Drug repositioning: identifying and developing new uses for existing drugs, *Nat Rev Drug Discov* 3, 673-683.
12. Ekins, S., Williams, A. J., Krasowski, M. D., and Freundlich, J. S. (2011) In silico repositioning of approved drugs for rare and neglected diseases, *Drug Discovery Today* 16, 298-310.
13. Liu, Z., Fang, H., Reagan, K., Xu, X., Mendrick, D. L., Slikker Jr, W., and Tong, W. (2013) In silico drug repositioning – what we need to know, *Drug Discovery Today* 18, 110-115.
14. Ma, D.-L., Chan, D. S.-H., and Leung, C.-H. (2013) Drug repositioning by structure-based virtual screening, *Chemical Society Reviews* 42, 2130-2141.
15. Bhakat, S., Karubiu, W., Jayaprakash, V., and Soliman, M. E. S. (2014) A perspective on targeting non-structural proteins to combat neglected tropical diseases: Dengue, West Nile and Chikungunya viruses, *European Journal of Medicinal Chemistry* 87, 677-702.
16. Guzman, M. G., Halstead, S. B., Artsob, H., Buchy, P., Farrar, J., Gubler, D. J., Hunsperger, E., Kroeger, A., Margolis, H. S., Martinez, E., Nathan, M. B., Pelegriano, J. L., Simmons, C., Yoksan, S., and Peeling, R. W. Dengue: a continuing global threat, *Nat Rev Micro*.
17. Bhatt, S., Gething, P. W., Brady, O. J., Messina, J. P., Farlow, A. W., Moyes, C. L., Drake, J. M., Brownstein, J. S., Hoen, A. G., Sankoh, O., Myers, M. F., George, D. B., Jaenisch, T., Wint, G. R. W., Simmons, C. P., Scott, T. W., Farrar, J. J., and Hay, S. I. (2013) The global distribution and burden of dengue, *Nature* 496, 504-507.
18. Guzman, M. G., and Harris, E. Dengue, *The Lancet* 385, 453-465.
19. Gubler, D. J. (1998) Dengue and Dengue Hemorrhagic Fever, *Clinical Microbiology Reviews* 11, 480-496.
20. Murrell, S., Wu, S.-C., and Butler, M. (2011) Review of dengue virus and the development of a vaccine, *Biotechnology Advances* 29, 239-247.
21. Wan, S.-W., Lin, C.-F., Wang, S., Chen, Y.-H., Yeh, T.-M., Liu, H.-S., Anderson, R., and Lin, Y.-S. (2013) Current progress in dengue vaccines, *Journal of Biomedical Science* 20, 37.
22. Rashad, A. A., Mahalingam, S., and Keller, P. A. (2014) Chikungunya virus: emerging targets and new opportunities for medicinal chemistry, *J Med Chem* 57, 1147-1166.
23. Schwartz, O., and Albert, M. L. (2010) Biology and pathogenesis of chikungunya virus, *Nat Rev Micro* 8, 491-500.
24. Staples, J. E., Breiman, R. F., and Powers, A. M. (2009) Chikungunya Fever: An Epidemiological Review of a Re-Emerging Infectious Disease, *Clinical Infectious Diseases* 49, 942-948.
25. Manns, M. P., and von Hahn, T. (2013) Novel therapies for hepatitis C [mdash] one pill fits all?, *Nat Rev Drug Discov* 12, 595-610.
26. Pokorná, J., Machala, L., Řezáčová, P., and Konvalinka, J. (2009) Current and Novel Inhibitors of HIV Protease, *Viruses* 1, 1209-1239.
27. Clercq, E. D. (2007) The design of drugs for HIV and HCV, *Nat Rev Drug Discov* 6, 1001-1018.
28. Noble, C. G., Seh, C. C., Chao, A. T., and Shi, P. Y. (2012) Ligand-bound structures of the dengue virus protease reveal the active conformation, *J Virol* 86, 438-446.
29. <http://www.rcsb.org/pdb/explore/explore.do?structureId=3TRK>.
30. Erbel, P., Schiering, N., D'Arcy, A., Rénatus, M., Kroemer, M., Lim, S. P., Yin, Z., Keller, T. H., Vasudevan, S. G., and Hommel, U. (2006) Structural basis for the activation of flaviviral NS3 proteases from dengue and West Nile virus, *Nat Struct Mol Biol* 13, 372-373.

31. <http://www.chemspider.com/>.
32. Maharaj, Y., Bhakat, S., and E. S. Soliman, M. (2015) Computer-aided Identification of Novel DprE1 Inhibitors as Potential Anti-TB Lead Compounds: A Hybrid Virtual-screening and Molecular Dynamics Approach, *Letters in Drug Design & Discovery* 12, 302-313.
33. Trott, O., and Olson, A. J. (2010) AutoDock Vina: improving the speed and accuracy of docking with a new scoring function, efficient optimization and multithreading, *Journal of Computational Chemistry* 31, 455-461.
34. Lau, C. D., Levesque, M. J., Chien, S., Date, S., and Haga, J. H. (2010) ViewDock TDW: high-throughput visualization of virtual screening results, *Bioinformatics* 26, 1915-1917.
35. Pettersen, E. F., Goddard, T. D., Huang, C. C., Couch, G. S., Greenblatt, D. M., Meng, E. C., and Ferrin, T. E. (2004) UCSF Chimera--a visualization system for exploratory research and analysis, *J Comput Chem* 25, 1605-1612.
36. Lyne, P. D., Lamb, M. L., and Saeh, J. C. (2006) Accurate Prediction of the Relative Potencies of Members of a Series of Kinase Inhibitors Using Molecular Docking and MM-GBSA Scoring, *Journal of Medicinal Chemistry* 49, 4805-4808.
37. Rastelli, G., Rio, A. D., Degliesposti, G., and Sgobba, M. (2010) Fast and accurate predictions of binding free energies using MM-PBSA and MM-GBSA, *Journal of Computational Chemistry* 31, 797-810.
38. Sun, H., Li, Y., Shen, M., Tian, S., Xu, L., Pan, P., Guan, Y., and Hou, T. (2014) Assessing the performance of MM/PBSA and MM/GBSA methods. 5. Improved docking performance using high solute dielectric constant MM/GBSA and MM/PBSA rescoring, *Physical Chemistry Chemical Physics* 16, 22035-22045.
39. Abdulhameed, M. D., Hamza, A., and Zhan, C. G. (2006) Microscopic modes and free energies of 3-phosphoinositide-dependent kinase-1 (PDK1) binding with celecoxib and other inhibitors, *J Phys Chem B* 110, 26365-26374.
40. Li, N., Ainsworth, R. I., Ding, B., Hou, T., and Wang, W. (2015) Using Hierarchical Virtual Screening To Combat Drug Resistance of the HIV-1 Protease, *J Chem Inf Model* 55, 1400-1412.
41. Greenidge, P. A., Kramer, C., Mozziconacci, J. C., and Sherman, W. (2014) Improving Docking Results via Reranking of Ensembles of Ligand Poses in Multiple X-ray Protein Conformations with MM-GBSA, *Journal of Chemical Information and Modeling* 54, 2697-2717.
42. Sirin, S., Kumar, R., Martinez, C., Karmilowicz, M. J., Ghosh, P., Abramov, Y. A., Martin, V., and Sherman, W. (2014) A Computational Approach to Enzyme Design: Predicting  $\omega$ -Aminotransferase Catalytic Activity Using Docking and MM-GBSA Scoring, *Journal of Chemical Information and Modeling* 54, 2334-2346.
43. Slynko, I., Scharfe, M., Rumpf, T., Eib, J., Metzger, E., Schüle, R., Jung, M., and Sippl, W. (2014) Virtual Screening of PRK1 Inhibitors: Ensemble Docking, Rescoring Using Binding Free Energy Calculation and QSAR Model Development, *Journal of Chemical Information and Modeling* 54, 138-150.
44. D.A. Case, V. Babin, J.T. Berryman, R.M. Betz, Q. Cai, D.S. Cerutti, T.E. Cheatham, III, T.A. Darden, R.E. Duke, H. Gohlke, A.W. Goetz, S. Gusarov, N. Homeyer, P. Janowski, J. Kaus, I. Kolossváry, A. Kovalenko, T.S. Lee, S. LeGrand, T. Luchko, R. Luo, B. Madej, K.M. Merz, F. Paesani, D.R. Roe, A. Roitberg, C. Sagui, R. Salomon-Ferrer, G. Seabra, C.L. Simmerling, W. Smith, J. Swails, R.C. Walker, J. Wang, R.M. Wolf, X. Wu and P.A. Kollman (2014), AMBER 14, University of California, San Francisco.
45. Bhakat, S., Martin, A. J. M., and Soliman, M. E. S. (2014) An integrated molecular dynamics, principal component analysis and residue interaction network approach reveals the impact of M184V mutation on HIV reverse transcriptase resistance to lamivudine, *Molecular BioSystems* 10, 2215-2228.

46. Roe, D. R., and Cheatham, T. E. (2013) PTRAJ and CPPTRAJ: Software for Processing and Analysis of Molecular Dynamics Trajectory Data, *Journal of Chemical Theory and Computation* 9, 3084-3095.
47. Humphrey, W., Dalke, A., and Schulten, K. (1996) VMD: Visual molecular dynamics, *Journal of Molecular Graphics* 14, 33-38.
48. Delang, L., Segura Guerrero, N., Tas, A., Querat, G., Pastorino, B., Froeyen, M., Dallmeier, K., Jochmans, D., Herdewijn, P., Bello, F., Snijder, E. J., de Lamballerie, X., Martina, B., Neyts, J., van Hemert, M. J., and Leyssen, P. (2014) Mutations in the chikungunya virus non-structural proteins cause resistance to favipiravir (T-705), a broad-spectrum antiviral, *J Antimicrob Chemother* 69, 2770-2784.
49. Kaptein, S. J. F., De Burghgraeve, T., Froeyen, M., Pastorino, B., Alen, M. M. F., Mondotte, J. A., Herdewijn, P., Jacobs, M., de Lamballerie, X., Schols, D., Gamarnik, A. V., Sztaricskai, F., and Neyts, J. (2010) A Derivate of the Antibiotic Doxorubicin Is a Selective Inhibitor of Dengue and Yellow Fever Virus Replication In Vitro, *Antimicrobial Agents and Chemotherapy* 54, 5269-5280.
50. Deng, J., Li, N., Liu, H., Zuo, Z., Liew, O. W., Xu, W., Chen, G., Tong, X., Tang, W., Zhu, J., Zuo, J., Jiang, H., Yang, C.-G., Li, J., and Zhu, W. (2012) Discovery of Novel Small Molecule Inhibitors of Dengue Viral NS2B-NS3 Protease Using Virtual Screening and Scaffold Hopping, *Journal of Medicinal Chemistry* 55, 6278-6293.
51. Takhampunya, R., Ubol, S., Houg, H. S., Cameron, C. E., and Padmanabhan, R. (2006) Inhibition of dengue virus replication by mycophenolic acid and ribavirin, *J Gen Virol* 87, 1947-1952.
52. Koes, D. R., and Camacho, C. J. (2012) ZINCPharmer: pharmacophore search of the ZINC database, *Nucleic Acids Research* 40, W409-W414.
53. Toma, S., Yamashiro, T., Arakaki, S., Shiroma, J., Maeshiro, T., Hibiya, K., Sakamoto, N., Kinjo, F., Tateyama, M., and Fujita, J. (2009) Inhibition of intracellular hepatitis C virus replication by nelfinavir and synergistic effect with interferon-alpha, *J Viral Hepat* 16, 506-512.
54. Kraus, M., Bader, J., Overkleeft, H., and Driessen, C. (2013) Nelfinavir augments proteasome inhibition by bortezomib in myeloma cells and overcomes bortezomib and carfilzomib resistance, *Blood Cancer Journal* 3, e103.
55. Nitsche, C., Schreier, V. N., Behnam, M. A., Kumar, A., Bartenschlager, R., and Klein, C. D. (2013) Thiazolidinone-peptide hybrids as dengue virus protease inhibitors with antiviral activity in cell culture, *J Med Chem* 56, 8389-8403.
56. Zhou, G. C., Weng, Z., Shao, X., Liu, F., Nie, X., Liu, J., Wang, D., Wang, C., and Guo, K. (2013) Discovery and SAR studies of methionine-proline anilides as dengue virus NS2B-NS3 protease inhibitors, *Bioorg Med Chem Lett* 23, 6549-6554.
57. Yildiz, M., Ghosh, S., Bell, J. A., Sherman, W., and Hardy, J. A. (2013) Allosteric inhibition of the NS2B-NS3 protease from dengue virus, *ACS Chem Biol* 8, 2744-2752.
58. Ganesh, V. K., Muller, N., Judge, K., Luan, C. H., Padmanabhan, R., and Murthy, K. H. (2005) Identification and characterization of nonsubstrate based inhibitors of the essential dengue and West Nile virus proteases, *Bioorg Med Chem* 13, 257-264.

### **Figure legends**

**Figure 1. I.** The active site region of the DENV NS2B-NS3 protease is delineated in red. **II.** The catalytic triad of the DENV NS2B-NS3 protease consists of His51 (B), Asp75 (A) and Ser135 (C). The ligand-bound closed conformation of the dengue NS2B-NS3 protease (PDB: 3U1I) was used to fathom the position of the active site and catalytic triad.

**Figure 2.** The active site region of the CHIKV NSP2 protease (PDB: 3TRK) is delineated in red. The conformation of the active site residues (in red) was deduced by running SiteHound and MetaPocket web servers (see Supplementary Materials).

**Figure 3.** The 2D structures of representative HIV/HCV protease inhibitors that were used in this drug repurposing study. A, B, C, D, E, F, G, H and I represents, respectively, lopinavir (LPV), nelfinavir (NFV), amprenavir (AMP), atazanavir (ATV), indinavir (IDV), ritonavir (RTV), saquinavir (SQV), telaprevir (TPV) and darunavir (DRV).

**Figure 4.** 2D representation of the structure of some previously-reported CHIKV NSP2 inhibitors; A and D represent the chemical structures of two CHIKV NSP2 inhibitors as predicted *in silico* by Rashad *et al*(22).

**Figure 5.** Chemical structures of some previously-reported DENV NS2B-NS3 protease inhibitors. **A.** R, R1 are the position of substitutions as reported by *Nitsche et al(55)*.; **B.** one of the anilide reported by *Zhou et al(56)*.; **C.** one of the promising NS2B-NS3 inhibitors reported by *Yildiz et al(57)*.; **D.** one of the potent DENV NS2B-NS3 inhibitor reported by *Ganesh et al(58)*.

**Figure 6.** The common peptidomimetic chemical similarity among HIV/HCV inhibitors, DENV NS2B-NS3 inhibitor/s and CHIKV NSP2 inhibitor/s inspired the repositioning concept.

**Figure 7.** Superimposed docked conformations of HIV/HCV inhibitors used in this study within the active site of DENV NS2B-NS3 protease (PDB: 3U11) and CHIKV NSP2 (PDB: 3TRK).

**Figure 8.** Dose response curves of the antiviral effect (black bars) and the cytotoxic effect (white circles) of **A)** lopinavir and nelfinavir in the chikungunya virus CPE reduction assay and **B)** lopinavir, nelfinavir and ritonavir in the dengue virus yield reduction assay.

**Figure 9A.** Ligand interaction map of NFV bound in the active site of the DENV NS2B-NS3 protease with indication of the different interactions between protein and inhibitor

**Figure 9B.** The putative position of the catalytic triad and nelfinavir (NFV) in the active site of DENV NS2B-NS3 protease.

**Figure 9C.** Per-residue footprint of active site residues involved in the interaction with nelfinavir. Highlighting electrostatic and van der Waals contributions coming from active site residues.

**Figure 10A.** Ligand interaction plot showing active site residues of C terminal CHIKV NSP2 with nelfinavir (NFV).

**Figure 10B.** Per-residue footprint of active site residues involved in the interaction with nelfinavir (NFV). Highlighting contributions coming from electrostatic and van der Waals interactions in case of each residue.

**Figure 10C.** The position of catalytic cysteine residues in the C-terminal domain and His1222 in respective with nelfinavir (NFV)

**Figure 11.** A and B highlights the minimum pharmacophore features of NFV in bound conformation with DENV NS2B-NS3 protease and CHIKV NSP2, respectively. The artistic representation of the common pharmacophore feature of NFV for their DENV/CHIKV protease activity is described with the arrows. The yellow highlighted region represents the core area of the peptidomimetic scaffold. Green, yellow and white regions of pharmacophore points

represents HP (hydrophobic), HB<sub>D</sub> (hydrogen bond donor), HB<sub>A</sub> (hydrogen bond acceptor) respectively.

### **Table legends**

**Table 1.** MM/GBSA based binding free energy profile in comparison with docking score for all re-profiled HIV/HCV inhibitors presented in this study.

**Table 2.** Antiviral activity of HIV/HCV protease inhibitors against DENV and CHIKV

**Table 3.** Average hydrogen bond distance (Å) and % occupancy of interacting active site residues with NFV during simulation time.

**Table 4.** Average hydrogen bond distance and % occupancy between –NH<sub>2</sub> side chain of His1222 and NFV.

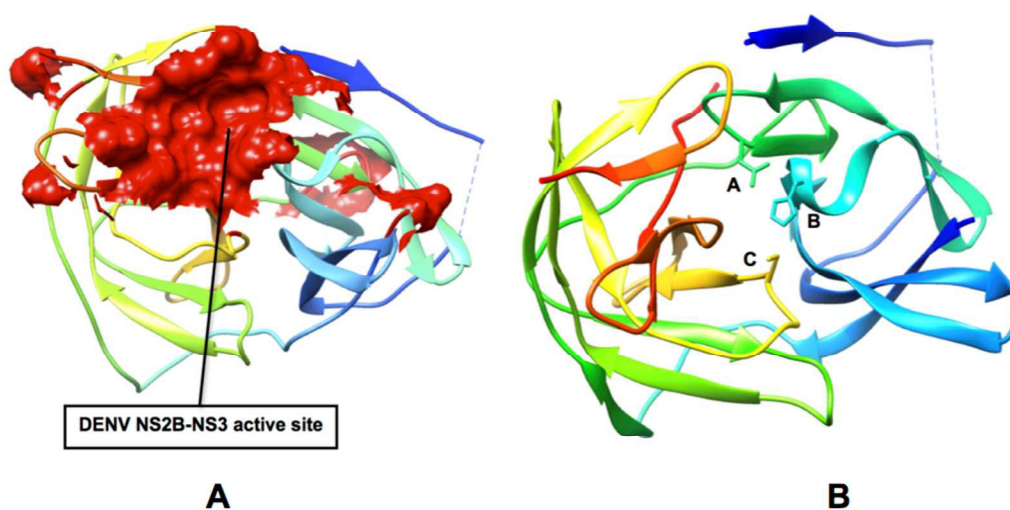


**Figure 1. I.** The active site region of the DENV NS2B-NS3 protease is delineated in red. **II.** The catalytic triad of the DENV NS2B-NS3 protease consists of His51 (B), Asp75 (A) and Ser135 (C). The ligand-bound closed conformation of the dengue NS2B-NS3 protease (PDB: 3U1I) was used to fathom the position of the active site and catalytic triad.

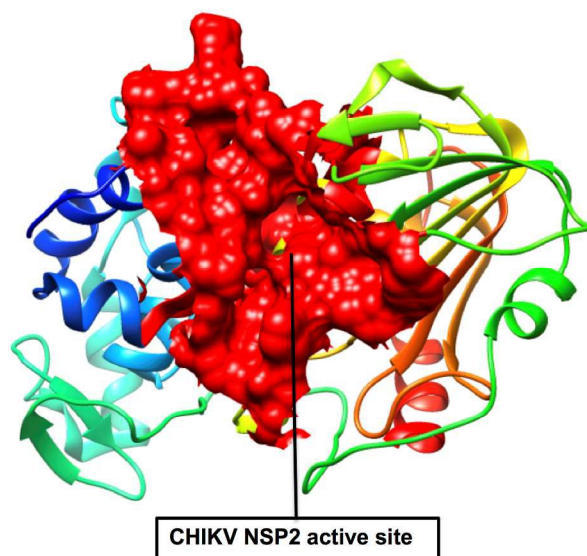


**Figure 2.** The active site region of the CHIKV NSP2 protease (PDB: 3TRK) is delineated in red. The conformation of the active site residues (in red) was deduced by running SiteHound and MetaPocket web servers (see Supplementary Materials).

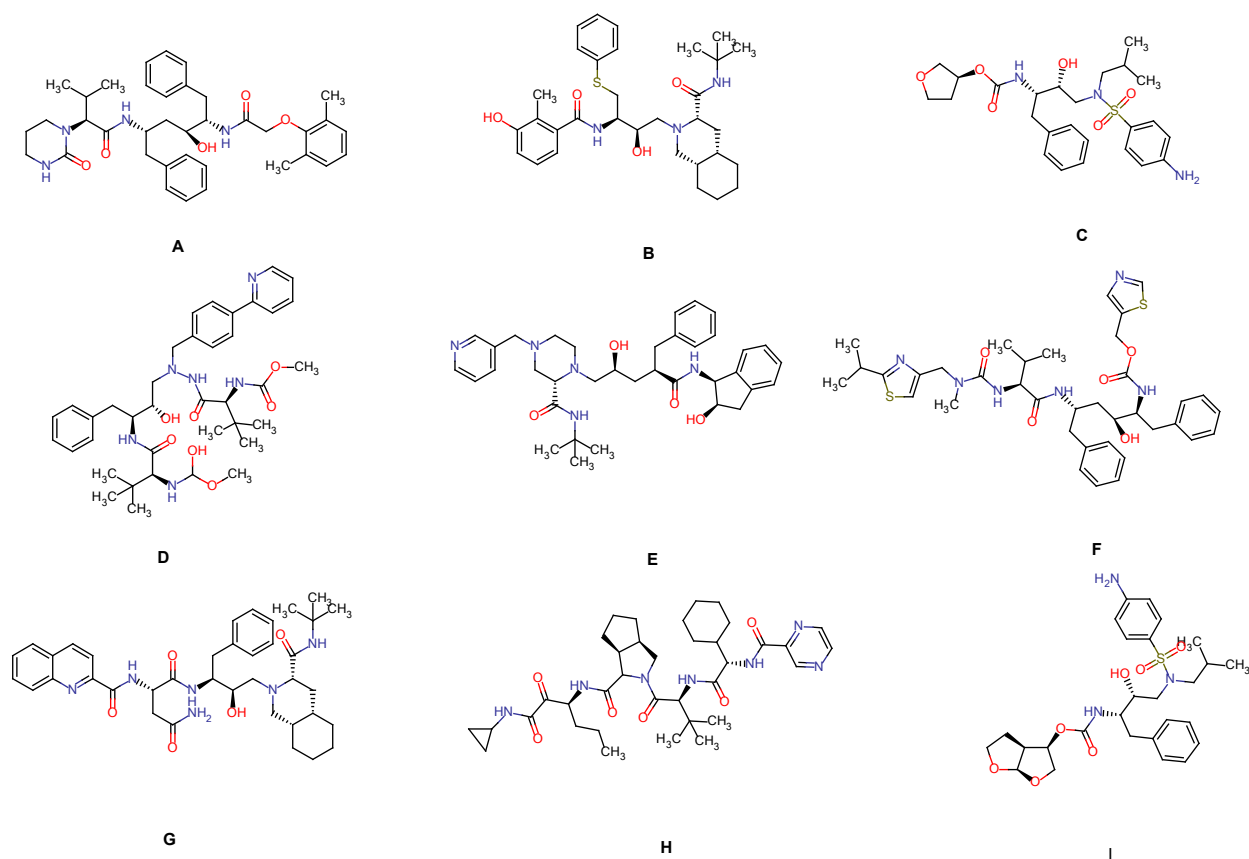


**Figure 3.** The 2D structures of representative HIV/HCV protease inhibitors that were used in this drug repurposing study. A, B, C, D, E, F, G, H and I represents, respectively, lopinavir (LPV), nelfinavir (NFV), amprenavir (AMP), atazanavir (ATV), indinavir (IDV), ritonavir (RTV), saquinavir (SQV), telaprevir (TPV) and darunavir (DRV).

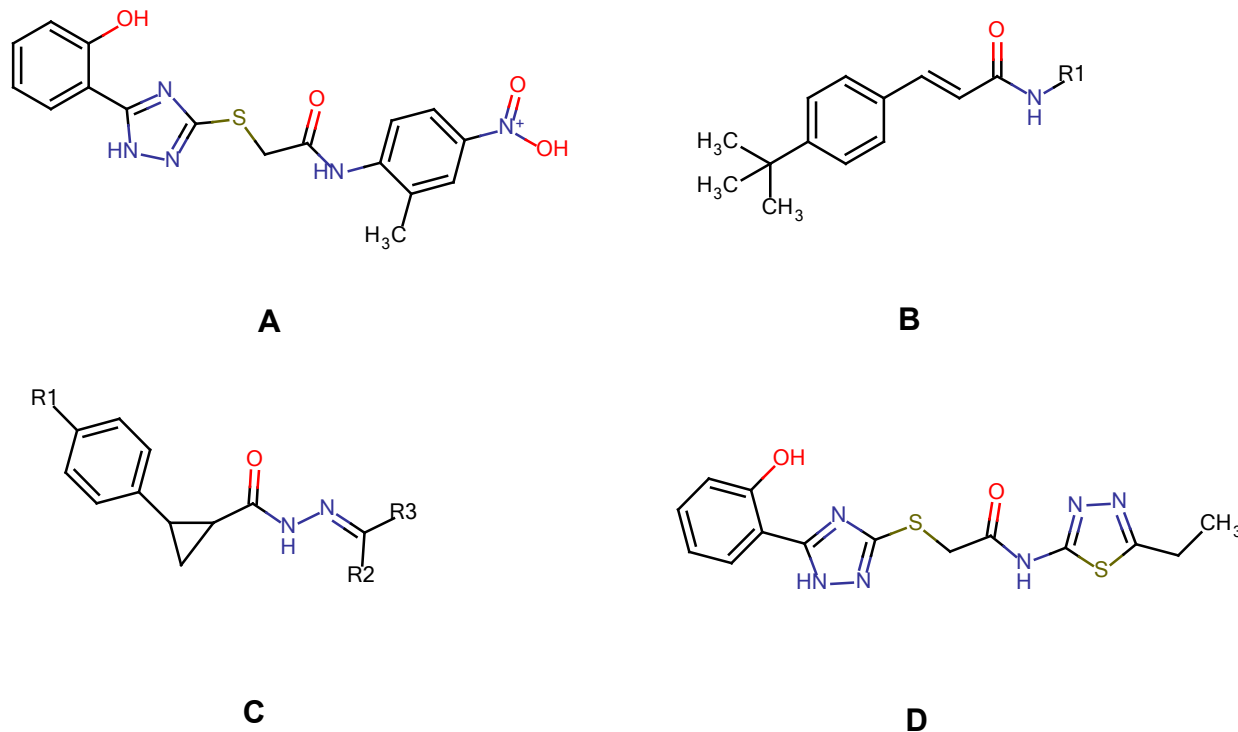


**Figure 4.** 2D representation of the structure of some previously-reported CHIKV NSP2 inhibitors; A and D represent the chemical structures of two CHIKV NSP2 inhibitors as predicted *in silico* by Rashad *et al*(22).

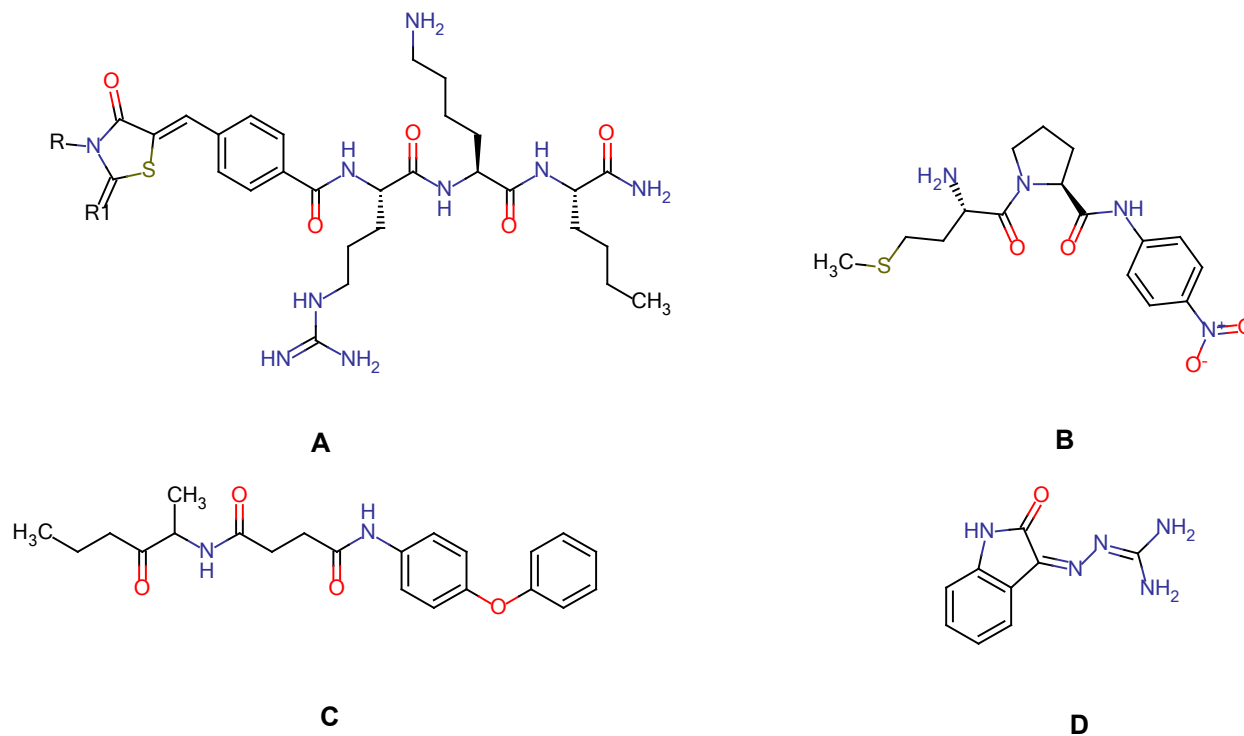


**Figure 5.** Chemical structures of some previously-reported DENV NS2B-NS3 protease inhibitors. **A.** R, R1 are the position of substitutions as reported by *Nitsche et al(55)*.; **B.** one of the anilide reported by *Zhou et al(56)*.; **C.** one of the promising NS2B-NS3 inhibitors reported by *Yildiz et al(57)*.; **D.** one of the potent DENV NS2B-NS3 inhibitor reported by *Ganesh et al(58)*.

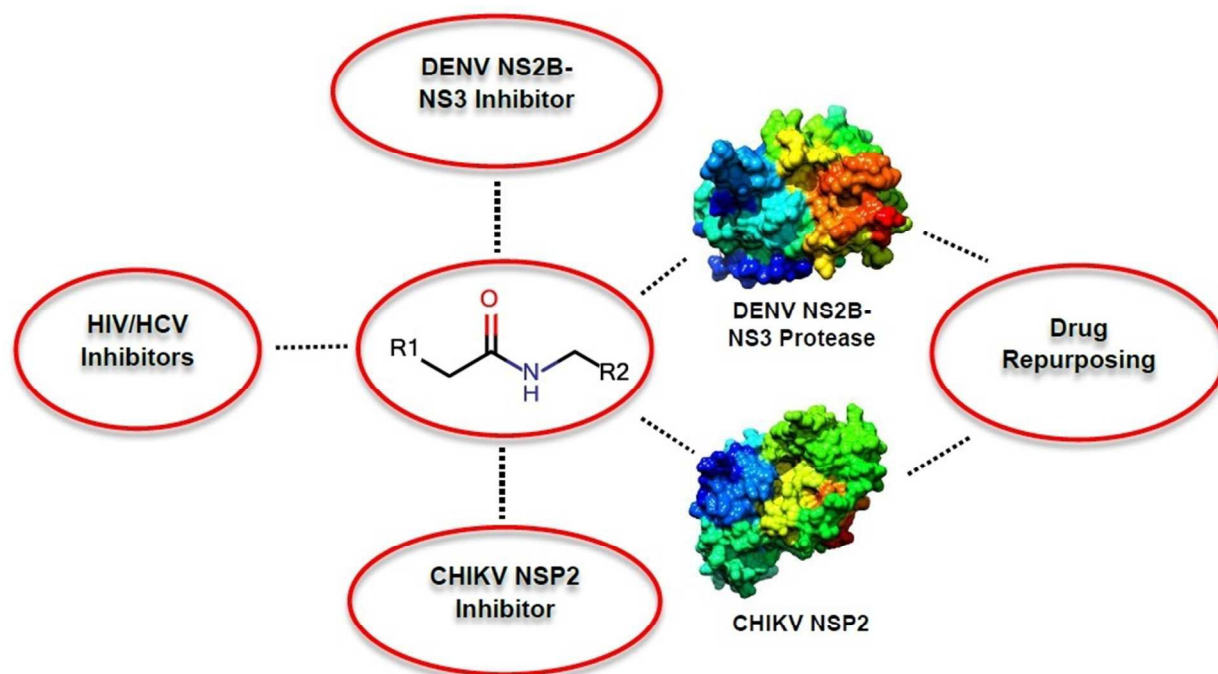


**Figure 6.** The common peptidomimetic chemical similarity among HIV/HCV inhibitors, DENV NS2B-NS3 inhibitor/s and CHIKV NSP2 inhibitor/s inspired the repositioning concept.

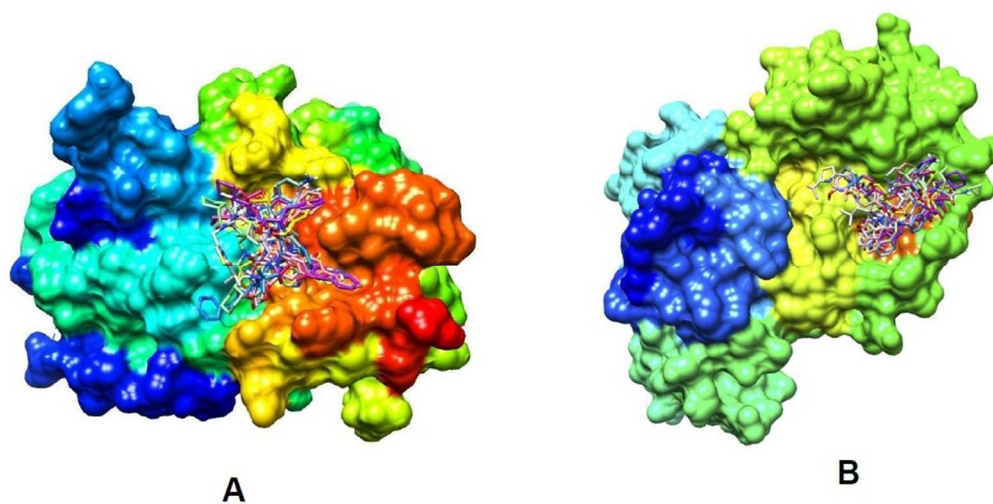


**Figure 7.** Superimposed docked conformations of HIV/HCV inhibitors used in this study within the active site of DENV NS2B-NS3 protease (PDB: 3U11) and CHIKV NSP2 (PDB: 3TRK).

A

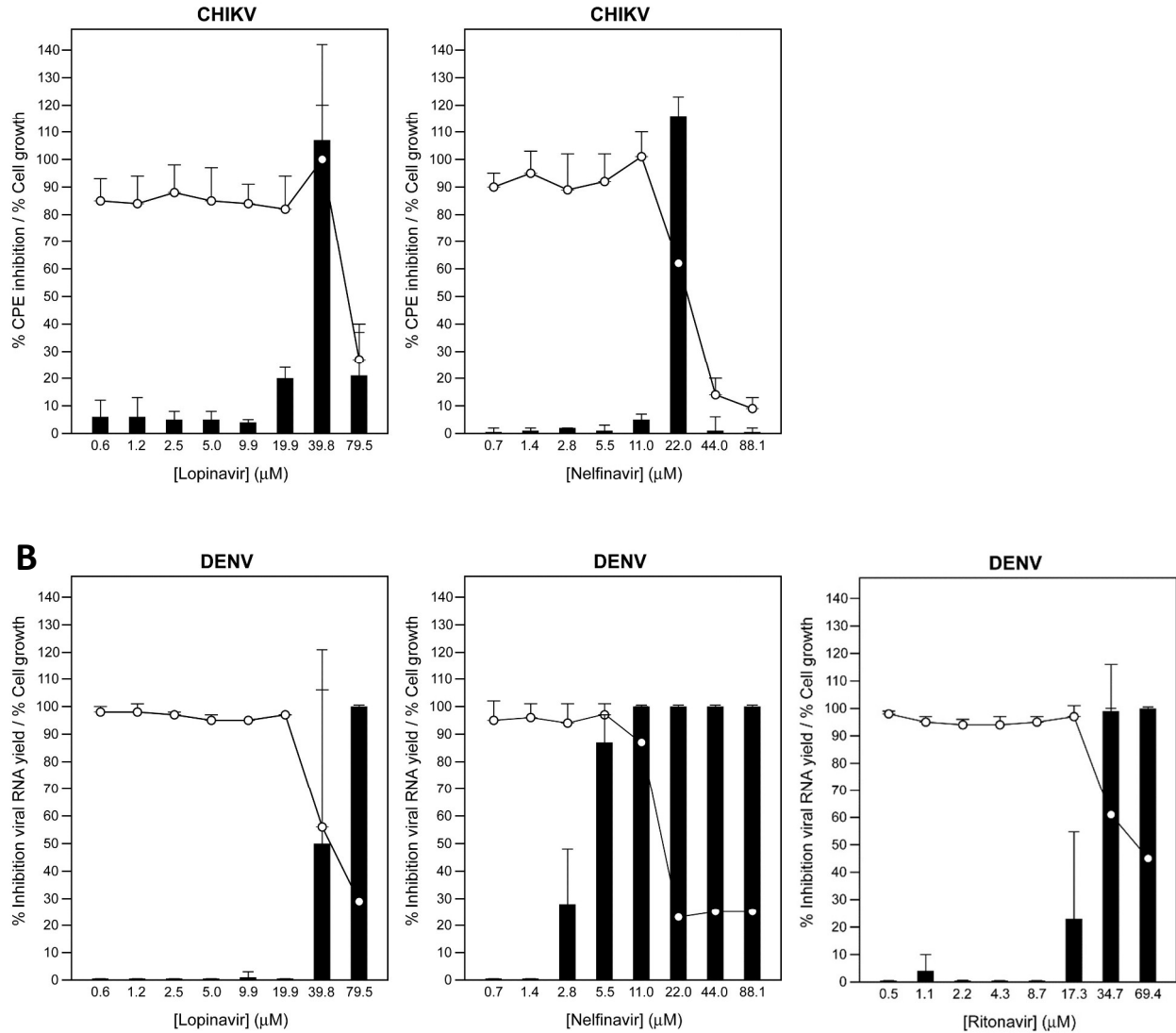


**Figure 8.** Dose response curves of the antiviral effect (black bars) and the cytotoxic effect (white circles) of **A)** lopinavir and nelfinavir in the chikungunya virus CPE reduction assay and **B)** lopinavir, nelfinavir and ritonavir in the dengue virus yield reduction assay.

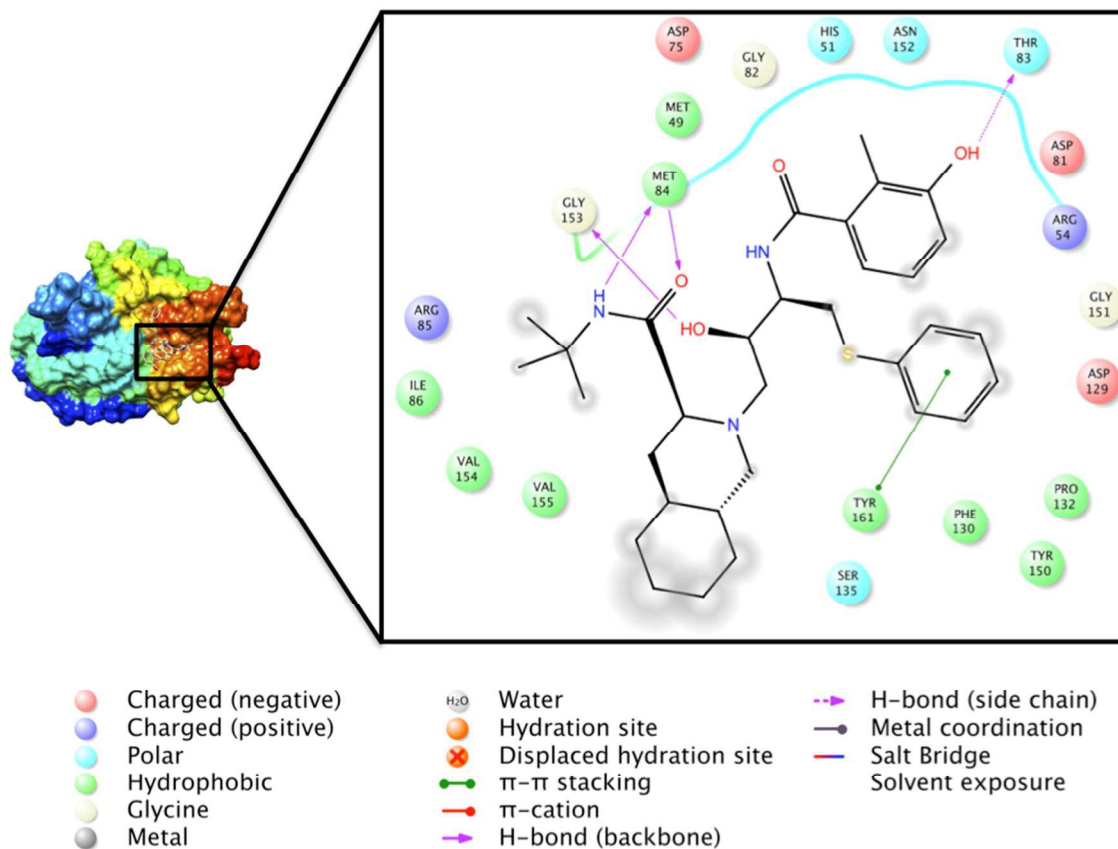


**Figure 9A.** Ligand interaction map of NFV bound in the active site of the DENV NS2B-NS3 protease with indication of the different interactions between protein and inhibitor

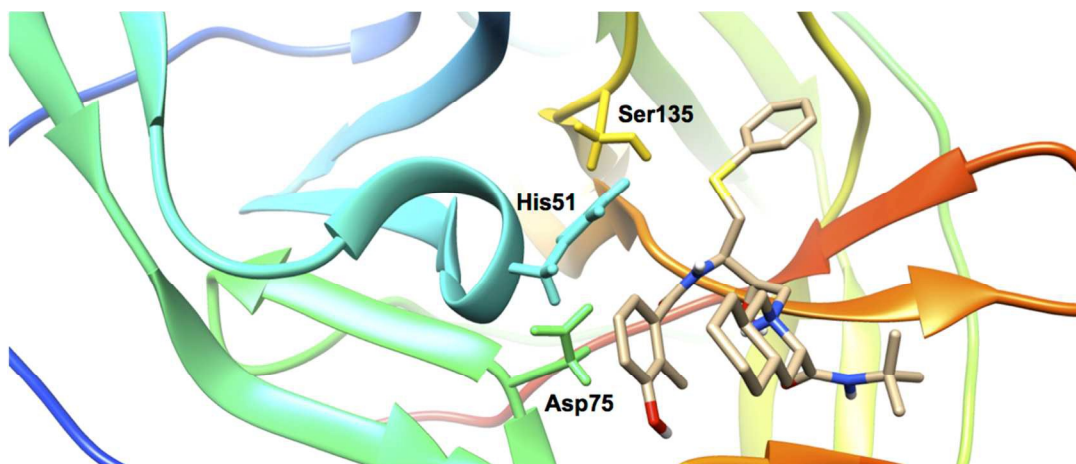


**Figure 9B.** The putative position of the catalytic triad and nelfinavir (NFV) in the active site of DENV NS2B-NS3 protease.

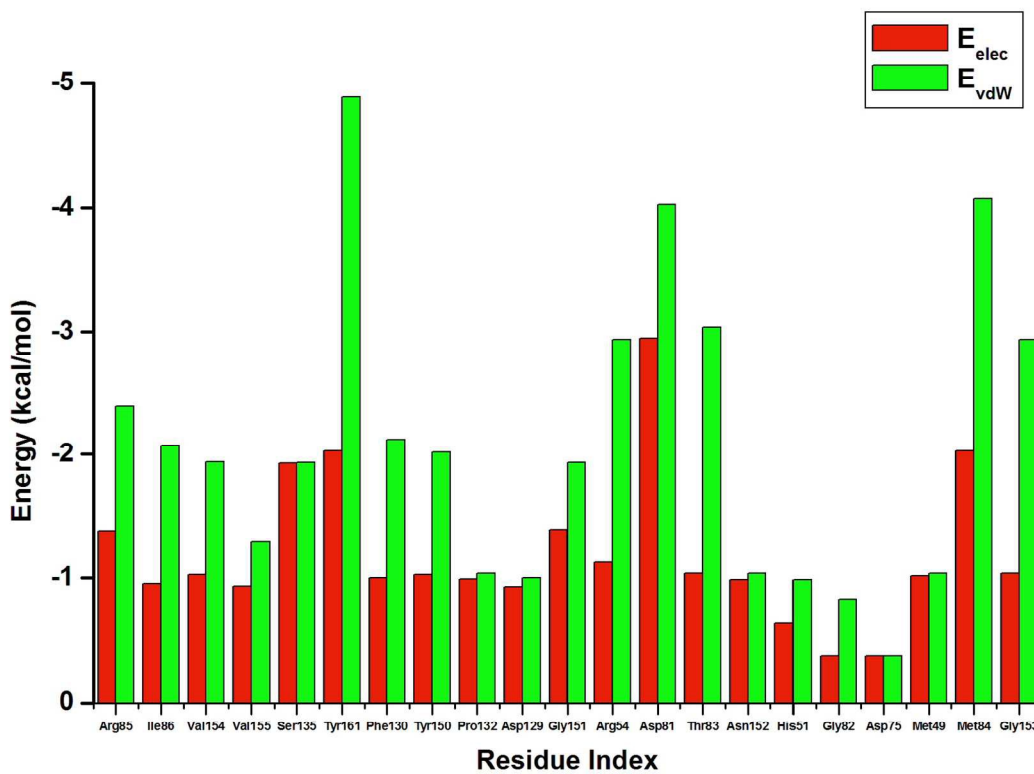


**Figure 9C.** Per-residue footprint of active site residues involved in the interaction with nelfinavir. Highlighting electrostatic and van der Waals contributions coming from active site residues.

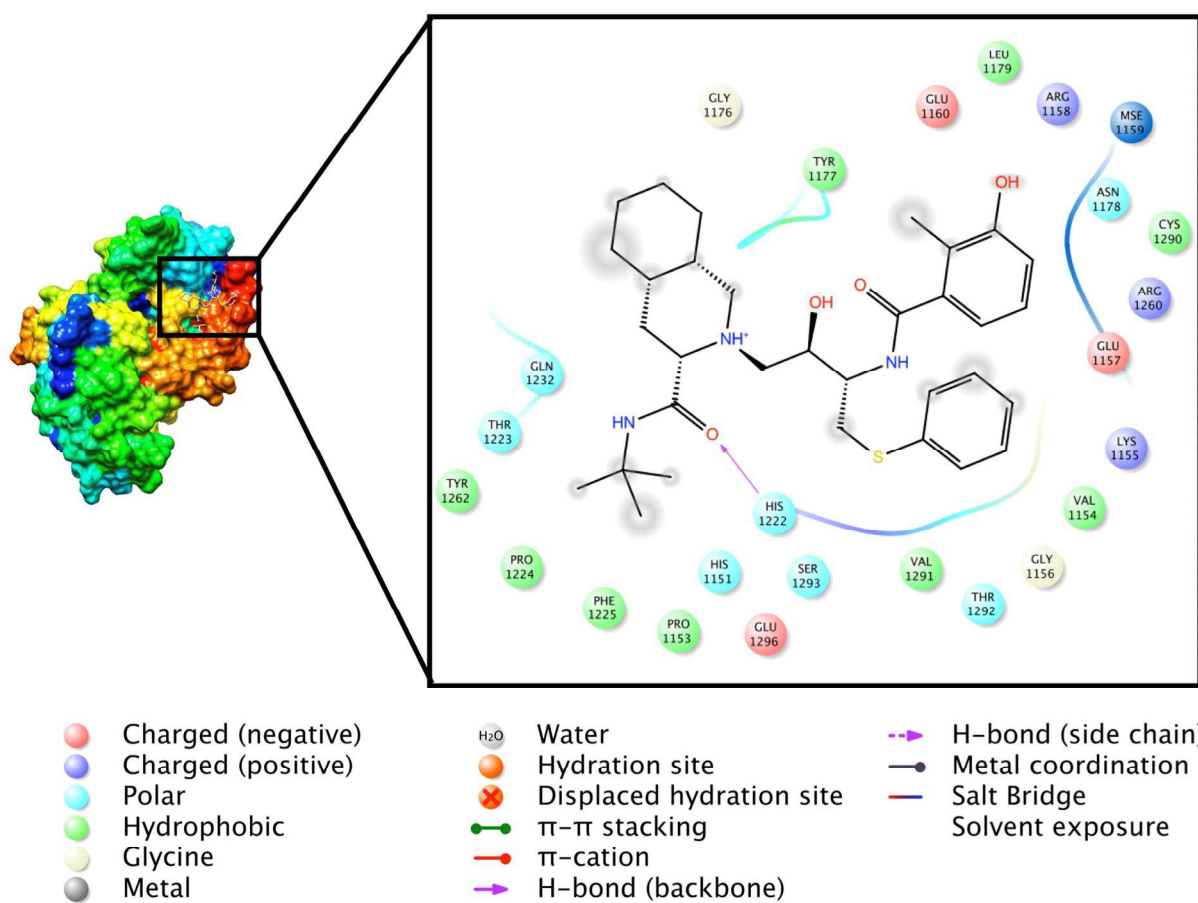


**Figure 10A.** Ligand interaction plot showing active site residues of C terminal CHIKV NSP2 with nelfinavir (NFV).

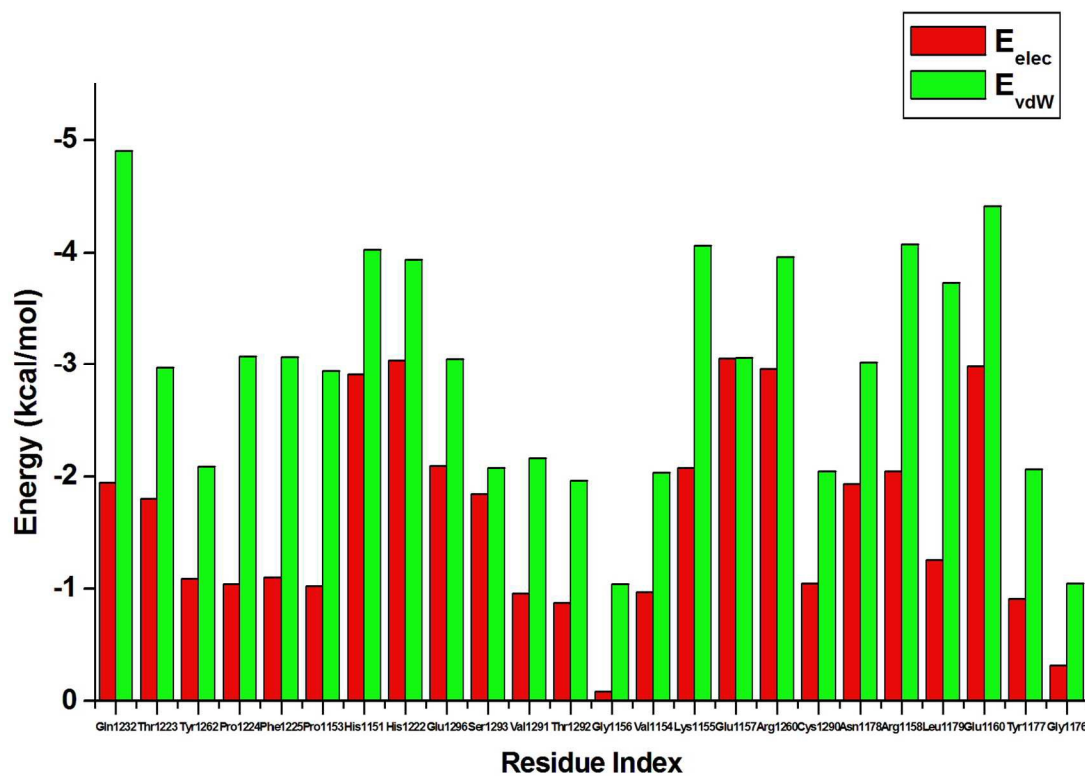


**Figure 10B.** Per-residue footprint of active site residues involved in the interaction with nelfinavir (NFV). Highlighting contributions coming from electrostatic and van der Waals interactions in case of each residue.

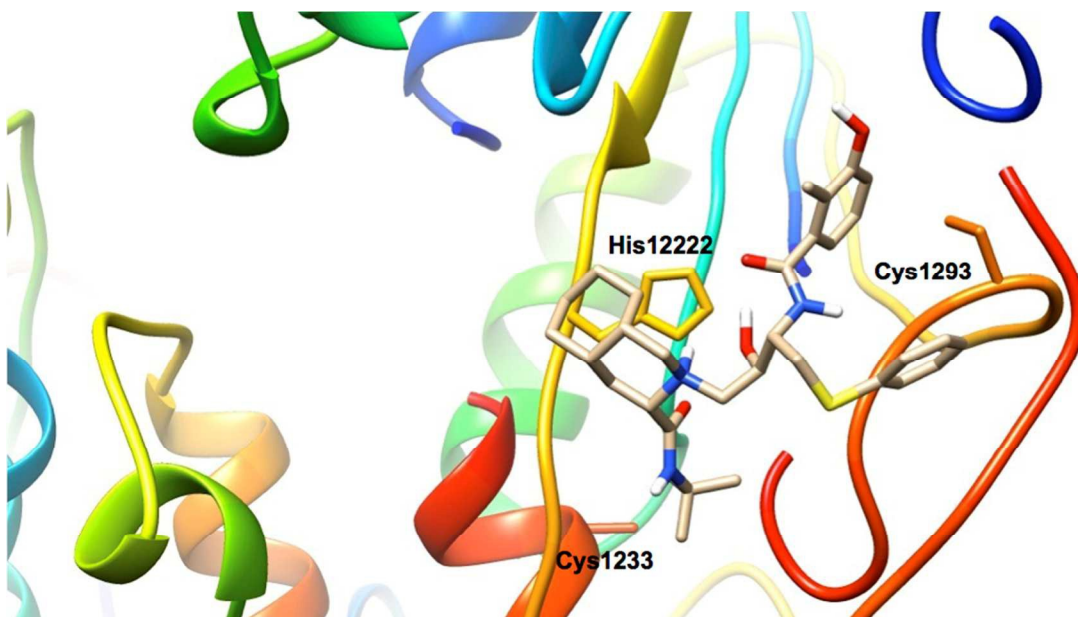


**Figure 10C.** The position of catalytic cysteine residues in the C-terminal domain and His1222 in respective with nelfinavir (NFV)

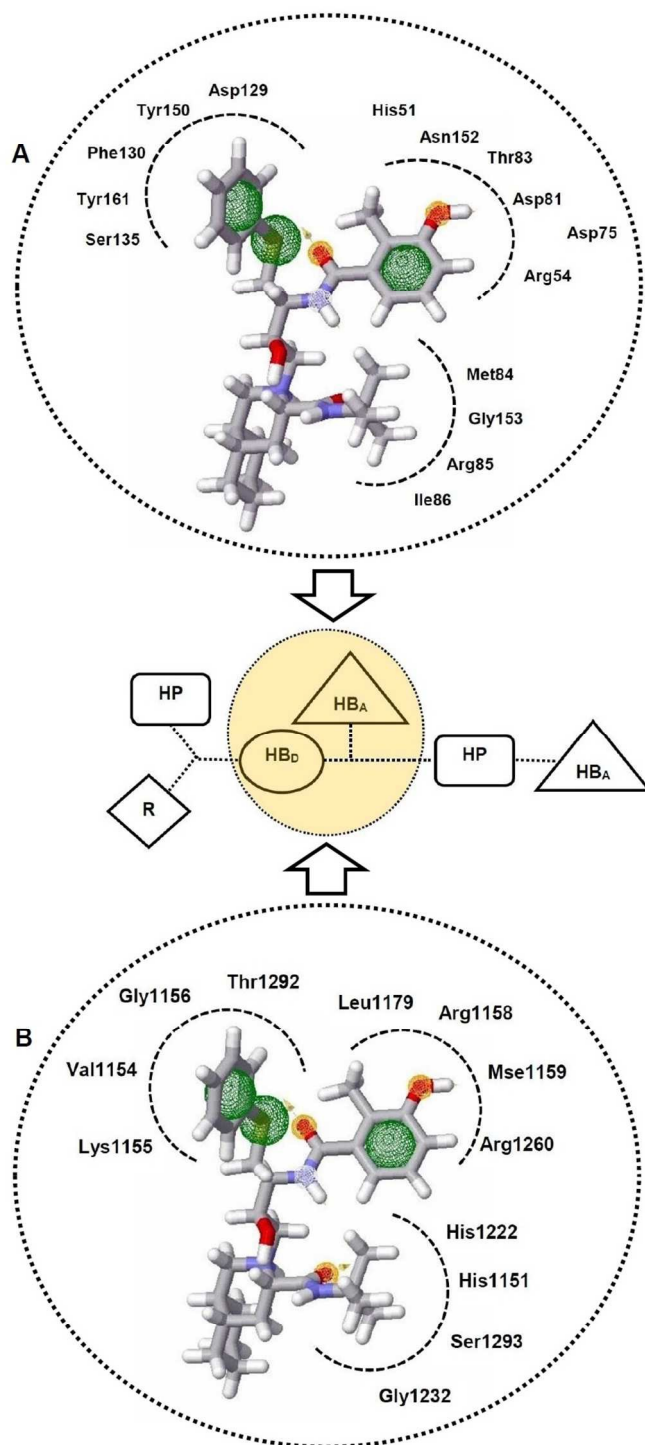


**Figure 11.** A and B highlights the minimum pharmacophore features of NFV in bound conformation with DENV NS2B-NS3 protease and CHIKV NSP2, respectively. The artistic

representation of the common pharmacophore feature of NFV for their DENV/CHIKV protease activity is described with the arrows. The yellow highlighted region represents the core area of the peptidomimetic scaffold. Green, yellow and white regions of pharmacophore points represents HP (hydrophobic), HB<sub>D</sub> (hydrogen bond donor), HB<sub>A</sub> (hydrogen bond acceptor) respectively.

**Table 1.** MM/GBSA based binding free energy profile in comparison with docking score for all re-profiled HIV/HCV inhibitors presented in this study

Ligand	E <sub>vdw</sub>	E <sub>elect</sub>	G <sub>gas</sub>	G <sub>solv</sub>	ΔG <sub>bind</sub>	Docking score
AMP	-29.6529±0.3262 <sup>†</sup>	0.0619±0.1230 <sup>†</sup>	-29.5911±0.3217 <sup>†</sup>	6.4800±0.1219 <sup>†</sup>	-23.1111±0.2546 <sup>†</sup>	-7.3 <sup>†</sup>
	-22.4738±0.3892*	-1.9473±0.2074*	-29.7597±0.5057*	12.1264±0.2073*	-12.2947±0.2037*	-6.3*
ATV	-38.0980±0.2978 <sup>†</sup>	-5.2609±0.2709 <sup>†</sup>	-	14.3965±0.2768 <sup>†</sup>	-22.9619±0.2981 <sup>†</sup>	-7.2 <sup>†</sup>
	-24.0476±0.6403*	-3.7475±0.6056*	43.3584±0.4630 <sup>†</sup> 6.7568±0.5067*	13.5103±0.3604*	-14.2848±0.2057*	-6.2*
RTV	-53.2588 ±0.2107 <sup>†</sup>	-2.6859 ±0.1617 <sup>†</sup>	-45.9456± 0.3144 <sup>†</sup>	13.9597±0.1536 <sup>†</sup>	-31.9859±0.2457 <sup>†</sup>	-8.6 <sup>†</sup>
	-23.9486±0.2011*	-3.8793±0.3810*	-35.8369±0.6037*	13.6207±0.4903	-14.2072±0.3803	-6.4*
LPV	-28.9049±0.5113 <sup>†</sup>	-8.9503 ±0.2415 <sup>†</sup>	-30.6537 ±0.6095 <sup>†</sup>	9.5843±0.2877 <sup>†</sup>	-28.2694±0.4378 <sup>†</sup>	-8.4 <sup>†</sup>
	-34.0582±0.3940*	-4.3948±0.2048*	-32.8653±0.3803*	15.9674±0.2047*	-22.4856±0.2710*	-6.2*
DRV	-32.5832±0.3492 <sup>†</sup>	-6.5005± 0.3255 <sup>†</sup>	-39.0837± 0.5231 <sup>†</sup>	16.3381±0.3074 <sup>†</sup>	-22.7456± 0.2876 <sup>†</sup>	-7.5 <sup>†</sup>
	-27.8572±0.4036*	-2.7578±0.9063*	-37.3605±0.5063*	18.0774±0.8057*	-12.5376±0.7485*	-6.6*
IDV	-33.9221±0.5955 <sup>†</sup>	-1.6321±0.9335 <sup>†</sup>	-28.7214±1.2058 <sup>†</sup>	12.1607±0.8491 <sup>†</sup>	-23.3925±0.8491 <sup>†</sup>	-7.1 <sup>†</sup>
	-22.8304±0.2907*	-1.3875±0.2038*	-28.8467±0.7073*	11.8232±0.4063	-12.3947±0.1078*	-6.6*
SQV	-38.2987±0.1778 <sup>†</sup>	-15.5666±0.5111 <sup>†</sup>	-25.9531±0.5245 <sup>†</sup>	25.4092±0.4550 <sup>†</sup>	-28.4561±0.1639 <sup>†</sup>	-7.6 <sup>†</sup>
	-28.7948±0.7207*	-3.4743±0.6749*	-30.9587±0.7064*	19.4018±0.6539*	-12.8673±0.3755*	-6.6*
NFV	-47.7996±0.2034 <sup>†</sup>	-12.1653±0.5720 <sup>†</sup>	-29.6342±0.5895 <sup>†</sup>	25.9687±0.5257 <sup>†</sup>	-33.9962±0.2118 <sup>†</sup>	-8.9 <sup>†</sup>
	-37.8567±0.2920*	-6.4839±0.2841*	-30.2874±0.3842*	19.4812±0.4201*	-24.8594±0.1047*	-6.7*
TPV	-41.3499±0.2826 <sup>†</sup>	-15.1257±0.0990 <sup>†</sup>	-42.4706±0.3000 <sup>†</sup>	28.2651±0.1136 <sup>†</sup>	-28.2055±0.2803 <sup>†</sup>	-7.6 <sup>†</sup>
	-26.8658±0.0637*	-4.8047±0.6862*	-36.7490±0.6402*	14.1308±0.8473*	-17.5397±0.2104*	-6.2*

<sup>†</sup> Indicates ligands complexed with DENV NS2B-NS3 (PDB: 3U11) whereas \* stands for ligands complexed with CHIKV NSP2 (PDB: 3TRK)

**Table 2.** Antiviral activity of HIV/HCV protease inhibitors against DENV and CHIKV

Protease inhibitors	Anti-DENV activity EC <sub>50</sub> (μM)	CC <sub>50</sub> (μM)	Anti-CHIKV activity EC <sub>50</sub> (μM)	CC <sub>50</sub> (μM)
Lopinavir	42 ± 20	47 ± 23	32 ± 9	44 ± 12
Nelfinavir	3.5 ± 0.4	16 ± 0.4	14 ± 1	22 ± 6
Amprenavir	> 49	> 49	> 99	> 99
Atazanavir	> 71	> 71	> 71	> 71

Indinavir	> 41	> 41	> 82	> 82
Ritonavir	22 ± 4.4	46 ± 27	> 69	53
Saquinavir	32 ± 7.7	> 37	> 75	54
Darunavir	> 84	> 84	> 84	> 84
Telaprevir	43 ± 10	> 50	> 50	> 50

**Table 3.** Average hydrogen bond distance (Å) and % occupancy of interacting active site residues with NFV during simulation time.

H-bond interaction	Average distance (Å)	% occupancy
Thr83 (OH)---(OH) NFV	2.31	81.3
Met 84 (NH <sub>2</sub> )---(O <sub>52</sub> ) NFV	3.12	85.2
Met 84 (O)---(NH) NFV	3.08	72.3
Gly 153 (O)---(OH) NFV	2.02	79.3

**Table 4.** Average hydrogen bond distance and % occupancy between –NH<sub>2</sub> side chain of His1222 and NFV.

H-bond interaction	Average distance (Å)	% occupancy
His1222 (NH <sub>2</sub> )---(O <sub>49</sub> ) NFV	3.50	88.2